JOURNAL OF AIRCRAFT
Vol. 41, No. 2, March–April 2004

Robust Wing Flutter Suppression Considering Aerodynamic Uncertainty

Dan Borglund* and Ulrik Nilsson†
Royal Institute of Technology, SE-100 44 Stockholm, Sweden

A robust aeroservoelastic stability analysis considering frequency-domain aerodynamic uncertainty is utilized for robust control law design for flutter suppression of a flexible wing. The problem of stabilizing the wing in flutter using a minimum amount of control power is posed. For this purpose, numerical optimization is used to minimize the norm of a simple low-order controller subject to constraints on robust closed-loop stability. Robust stability is enforced in the optimization problem by posing constraints on the upper bounds on structured singular values and eigenvalues obtained from a linear stability analysis. The resulting controller is synthesized using gain scheduling, and robust wing flutter suppression is demonstrated in wind-tunnel testing.

Introduction

THE need for taking uncertainties into account in aeroservoelastic analysis and design optimization has been evident for quite some time.[1] In the most unfavorable scenario, even the smallest discrepancy between a numerical model and the real system may cause significant performance degradations in practice.[2] The fact that every numerical model of a real system suffers from some level of uncertainty must, therefore, be taken into account in procedures for optimal design.

The methods available for robust control design have been successfully applied to aeroservoelastic problems. One such case is reported by Waszak,[3] where a μ-synthesis control system design is used for flutter suppression of a wind-tunnel model. In that particular study, a fairly simple uncertainty representation proved useful, which cannot be expected in general. Methods in which the structure of the control system is part of the design also tend to result in complex high-order controllers, which may not be required to meet the control objective. A recent application to aeroservoelastic design is presented by Moulin et al.,[4] where a μ-synthesis control system design is mediated with a structural optimization for optimal design of a wing structure.

Lind and Brenner[1] have demonstrated the use of structured singular value analysis (or μ analysis) for robust aeroservoelastic stability analysis. The multidisciplinary analysis is then completed with a description of the system uncertainties, and the worst-case critical load is computed subject to the specified uncertainty. Consequently, the usefulness of a robust multidisciplinary analysis not only depends on the accuracy of the disciplinary analyses, but also on the availability of a representative uncertainty description. In this paper, this approach is utilized to demonstrate the possibility to tailor directly the properties of an aeroservoelastic system subject to a detailed uncertainty description.

In aeroservoelastic analysis, the modeling of unsteady aerodynamic forces is undoubtedly the primary source of uncertainty. This was emphasized in a previous study by Borglund,[5] where an uncertainty description for slender-wing aerodynamics was developed. The practical usefulness of the uncertainty description was demonstrated by performing a robust aeroelastic stability analysis of a wind-tunnel model. This paper is a direct continuation of this work, where the developed analysis is utilized for robust control law design for flutter suppression. In the following, the robust aeroservoelastic stability analysis is outlined in some detail along with an optimization-based low-order controller design and closed-loop wind-tunnel testing.

Received 26 August 2002; revision received 8 July 2003; accepted for publication 11 July 2003.

*Research Associate, Department of Aeronautical and Vehicle Engineering, Divison of Flight Dynamics, Teknikringen 8. Member AIAA.

†Ph.D. Student, Department of Aeronautical and Vehicle Engineering, Division of Flight Dynamics, Teknikringen 8. Student Member AIAA.

Aeroservoelastic Plant

The wind-tunnel experiment considered by Borglund[5] is revisited. As shown in Fig. 1, a flexible wing with a controllable trailing-edge flap is subjected to unsteady aerodynamic loads in a low-speed wind tunnel at the Royal Institute of Technology. The elastic deformations, in terms of out-of-plane deflections at four different locations on the wing, are monitored in real time by an optical measurement system and fed back to a simple control system.

The development of a quite accurate aeroelastic analysis for small-amplitude motion of the wing is already presented by Borglund,[5] and the results will only be summarized here. When a modal formulation based on finite beam element structural analysis and lifting-line unsteady aerodynamics is used, the Laplace domain equations of motion can be written in the form

$$\boldsymbol{Q}(p, V)\boldsymbol{\eta}(p) = \boldsymbol{q}(p, V)\beta(p) \tag{1}$$

$$\boldsymbol{y}(p) = \boldsymbol{C}\boldsymbol{\eta}(p) \tag{2}$$

where the input $\beta(p)$ is the Laplace transformation of the flap deflection, $\boldsymbol{\eta}(p)$ the transformation of the vector of modal coordinates, and p the Laplace variable. The Laplace variable can be written $p = \sigma + i\omega$, where σ is the damping and ω the angular frequency of the motion. The transfer function matrix $\boldsymbol{Q}(p, V)$ accounts for inertial, elastic, and aerodynamic forces due to wing motion, whereas the vector $\boldsymbol{q}(p, V)$ accounts for inertial and aerodynamic forces due to flap motion, where V denotes the freestream airspeed. Finally, the vector with the four measured wing deflections $\boldsymbol{y}(p)$ is related to the modal coordinates through the output matrix $\boldsymbol{C}$.

In this study, the dynamic aeroelastic performance of the wing will be improved by active control of the flap. A simple low-order controller is used for this purpose, giving a feedback control law in the form

$$\beta(p) = \boldsymbol{K}[p, \boldsymbol{x}(V)]\boldsymbol{y}(p) \tag{3}$$

where the controller $\boldsymbol{K}[p, \boldsymbol{x}(V)]$ depends on a set of feedback gain variables $\boldsymbol{x}(V)$, which are scheduled with airspeed. When actuator dynamics and dynamics inherent to the digital control system are included, the controller can be written

$$\boldsymbol{K}[p, \boldsymbol{x}(V)] = K_a(p)K_s(p)K_d(p)\boldsymbol{K}_p[p, \boldsymbol{x}(V)] \tag{4}$$

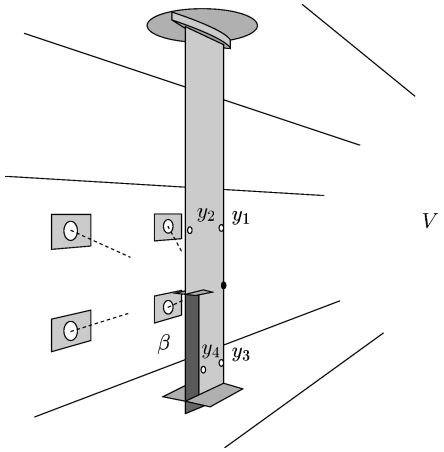

Fig. 1 Schematic layout of the wind-tunnel experiment.

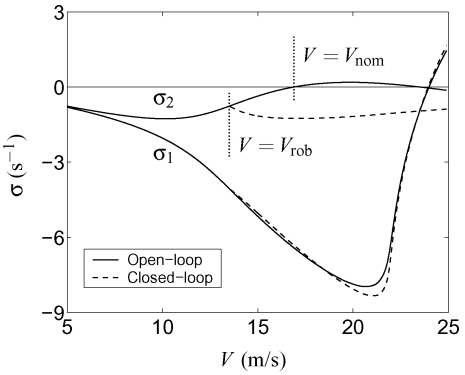

Fig. 2 Real part of the critical open- and closed-loop *p–k* eigenvalues vs airspeed.

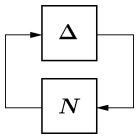

Fig. 3 Block diagram illustrating the uncertain closed-loop equations of motion as a feedback connection.

where $\boldsymbol{K}_p[p, \boldsymbol{x}(V)]$ represents the programmable part, $K_a(p) = \omega_0^2/(p^2 + 2\zeta\omega_0 p + \omega_0^2)$ the actuator servodynamics, $K_d(p) = e^{-pT}$ a computational delay of T seconds, and $K_s(p) = (1 - e^{-ph})/ph$ a sample-and-hold process with a sampling period of h seconds (Ref. 6). The values of all parameters in the defined transfer functions can be found by Borglund and Kuttenkeuler.[7]

For the programmable part of the controller, a simple wash-out filter structure[6]

$$\boldsymbol{K}_p[p, \boldsymbol{x}(V)] = \frac{p/\omega_P}{1 + p/\omega_P}\boldsymbol{x}_P^T(V) + \frac{p/\omega_D}{1 + p/\omega_D}\boldsymbol{x}_D^T(V) \qquad (5)$$

is chosen. If the values of the real filter parameters ω_P and ω_D are chosen small and large compared to the considered bandwidth, respectively, the controller will approximately behave like a proportional–derivative output feedback controller with four proportional feedback gains in the vector $\boldsymbol{x}_P(V)$ and four derivative feedback gains in the vector $\boldsymbol{x}_D(V)/\omega_D$. For a given airspeed V, the controller dynamics is, thus, determined by eight feedback gains in the vector

$$\boldsymbol{x}(V) = \begin{bmatrix} \boldsymbol{x}_P(V) \\ \boldsymbol{x}_D(V) \end{bmatrix} \qquad (6)$$

of control system design variables.

Based on the quality of the displacement measurements, which were found to have a very low level of noise, the filter parameters were set to $\omega_P = 10$ rad/s and $\omega_D = 400$ rad/s. For finite values of the feedback gains, the resulting controller has a zero steady-state gain ($\boldsymbol{K}[p, \boldsymbol{x}(V)] \to \boldsymbol{0}$ as $p \to 0$) and will, thus, not respond to static aeroelastic deformation. The controller also has a finite ∞ norm and the maximum gain is achieved at a finite frequency because $\boldsymbol{K}[p, \boldsymbol{x}(V)] \to \boldsymbol{0}$ as $p \to \infty$ due to the rolloff provided by the actuator dynamics. Based on this, the ∞ norm of the controller will be used as a measure of control power.

Nominal Stability Analysis

The closed-loop Laplace-domain equations of motion, obtained by inserting the control law Eq. (3) in Eqs. (1) and (2), can be posed as the nonlinear eigenvalue problem,

$$\{\boldsymbol{Q}(p, V) - \boldsymbol{q}(p, V)\boldsymbol{K}[p, \boldsymbol{x}(V)]\boldsymbol{C}\}\boldsymbol{\eta}(p) = \boldsymbol{0} \qquad (7)$$

Provided that the eigenvalue problem Eq. (7) can be posed and solved (which requires aerodynamic forces in the Laplace domain), the system is stable if all eigenvalues p have a negative real part σ. However, stability of an aeroservoelastic system is most commonly determined by considering the eigenvalues of a *p–k* approximation of the Laplace-domain equations of motion,[8] which only requires aerodynamic forces in the frequency domain. A *p–k* stability analysis provides approximate eigenvalues p for subcritical airspeeds, but any critical *p–k* eigenvalue, $p = i\omega$, is also a solution to Eq. (7).[5] This means that the prediction of the stability boundary is not compromised by the *p–k* approximation. Now, for a given control law $\boldsymbol{x}(V)$, the critical airspeed is computed by increasing the airspeed until some *p–k* eigenvalue p crosses the stability boundary $\sigma = 0$. At this speed, the mode corresponding to the critical eigenvalue, $p = i\omega$, displays self-sustained oscillations with angular frequency ω.

The open-loop stability is investigated by simply setting $\boldsymbol{x}(V) = \boldsymbol{0}$. The real part of the two relevant open-loop *p–k* eigenvalues are shown vs airspeed in Fig. 2 (solid lines). The wing is predicted to suffer a 6.3-Hz flutter instability in the second mode at the nominal flutter speed $V_{\text{nom}} = 16.9$ m/s. This agrees very well with the wind-tunnel experiment, where a 6.4-Hz flutter instability develops at $V_{\text{exp}} = 16.0$ m/s in the predicted mode. Furthermore, the first mode suffers a 2.8-Hz flutter instability at $V = 24.0$ m/s, and divergence occurs at $V_{\text{div}} = 24.5$ m/s according to the modal analysis.

Robust Stability Analysis

In a previous study,[5] it was argued that the discrepancies between the numerical and experimental open-loop results, although acceptable, are due to uncertain aerodynamic forces. An uncertainty description considering variations in magnitude, phase shift, and shape of the modal aerodynamic load distributions was developed. The uncertainty description was also validated[9] against experimental frequency-response data, and the result could be interpreted as if a 13% uncertainty in the unsteady aerodynamic forces was required to validate the uncertain model.

Without getting into details already accounted for in the previous study,[5] the developed uncertainty description can be written in the form of uncertain aerodynamic transfer function matrices. In the present notation, the transfer function matrices in Eq. (1) will then depend linearly on a set of complex parameters δ_j, $j = 1, \ldots, n_\delta$, which are only known by their scaled upper bounds $|\delta_j| \le 1$. When the very same procedure as outlined by Borglund[5] is used, the uncertain closed-loop equations of motion can be posed as the feedback connection in Fig. 3. For the present uncertainty description, the uncertain matrix $\boldsymbol{\Delta}$ is diagonal with multiples of the parameters δ_j on the diagonal.[5] Note that according to the bounds $|\delta_j| \le 1$ the uncertain system has been scaled such that $||\boldsymbol{\Delta}||_\infty \le 1$. Given the uncertain closed-loop equations of motion, it is a fairly straightforward matter to derive formally the corresponding transfer function matrix $\boldsymbol{N}[p, V, \boldsymbol{x}(V)]$ (Ref. 5).

Provided that the closed-loop system is nominally stable at a particular airspeed V, which is true if all eigenvalues of Eq. (7) have a negative real part, the wing is robustly stable subject to the

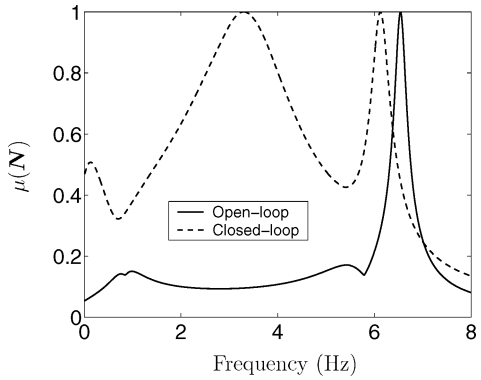

Fig. 4 Upper bound on $\mu[N(i\omega, V, x(V)]$ vs frequency; open-loop at $V = 13.5$ m/s and closed-loop at $V = 21.8$ m/s.

aerodynamic uncertainty if the structured singular value (SSV)

$$\mu\{\boldsymbol{N}[i\omega, V, \boldsymbol{x}(V)]\} < 1 \tag{8}$$

for all frequencies $\omega \geq 0$ (Ref. 1). Computing the SSV of a matrix subject to a given uncertainty set $\boldsymbol{\Delta}$ is unfortunately nontrivial.[10] In practice, upper and lower bounds on the SSV are considered to investigate criteria such as Eq. (8).

Robust stability of the open-loop system is now investigated by setting $\boldsymbol{x}(V) = \boldsymbol{0}$ in Eq. (8). As shown in Fig. 4 (solid line) the robust flutter analysis reveals that there is a potential risk for a flutter instability in the 6.5-Hz range from $V_{\text{rob}} = 13.5$ m/s and higher. As concluded by Borglund,[5] the robust flutter analysis is, with some amount of conservatism, capable of predicting the flutter instability observed in the experiment.

Control Law Design

The objective in this study is to suppress the second-mode flutter instability with a minimum amount of control power. According the nominal analysis, no control is required until $V_{\text{nom}} = 16.9$ m/s, whereas the wing becomes unstable at $V_{\text{exp}} = 16.0$ m/s in the experiment. Consequently, a control law design based on the nominal analysis would fail. However, according to the robust analysis, control is required from $V_{\text{rob}} = 13.5$ m/s, and a robust control law design is more likely to succeed.

For a fixed airspeed V, the problem of robustly stabilizing the wing using a minimum amount of control power can now, at least formally, be posed as the nonlinear programming problem

$$\min_{\boldsymbol{x}, z \geq 0} z \tag{9}$$

$$||\boldsymbol{K}(i\omega_j, \boldsymbol{x})||_2^2 \leq z^2, \qquad j = 1, \ldots, n_K \tag{10}$$

$$\mu(\boldsymbol{N}(i\omega_k, V, \boldsymbol{x})) \leq 1, \qquad k = 1, \ldots, n_\mu \tag{11}$$

$$\sigma_l(V, \boldsymbol{x}) \leq 0, \qquad l = 1, \ldots, n_p \tag{12}$$

where $\boldsymbol{x}$ is the vector of feedback gain design variables. The problem has been discretized such that the slack variable $z \geq 0$ represents the upper bound on the 2 norm of the controller frequency-response matrix for a discrete set of frequencies ω_j, $j = 1, \ldots, n_K$. If the chosen frequency range covers the peak value of $||\boldsymbol{K}(i\omega, \boldsymbol{x})||_2$, then the value of z at optimum represents $||\boldsymbol{K}(p, \boldsymbol{x})||_\infty$ to within discretization errors. In the same manner, the constraints in Eq. (11) constitute a discrete representation of the robust stability criterion Eq. (8), for which a second set $\omega_k, k = 1, \ldots, n_\mu$, of discrete frequencies is used. Finally, nominal stability is enforced by constraining the real parts $\sigma_l, l = 1, \ldots, n_p$, of the relevant closed-loop p–k eigenvalues.

Solving the optimization problem Eqs. (9)–(12) for a discrete set of airspeeds V_i, $i = 1, \ldots, n_V$, provides a set of optimal feedback gains $\boldsymbol{x}_i^*(V_i)$, which can be used for gain scheduling in the experiment. A potential difficulty regarding the continuity of the optimal control law $\boldsymbol{x}^*(V)$ is the existence of several local optima. Although it is not possible to show global optimality, it may be possible to track a specific local minima with airspeed such that a continuous high-performing control law is obtained.

Also note that the derivatives of the eigenvalue constraints Eq. (12) do not exist when there are coalescing eigenvalues,[11] making the problem nonsmooth. However, if the eigenvalues are distinct at the optimum, the problem can usually be solved using gradient-based optimization methods. The SSV for complex uncertainty, which is the case here, can be shown to be continuous in $\boldsymbol{N}$ (Ref. 12). However, the procedures for computing upper bounds on the SSV typically involves singular value analysis, which is founded on eigenvalue analysis. Possible difficulties related to the analytical and numerical properties of the constraint functions in Eqs. (11) and (12) will not be further emphasized in this study. Instead, focus is put on solving the particular problem at hand and verifying the performance of the optimal design in wind-tunnel testing.

The optimization problem Eqs. (9–12) was solved using the sequential quadratic programming routine implemented in the MATLAB® software.[13] The default settings with finite difference approximations for the derivatives of the constraint functions were used, giving a constraint violation of less than 10^{-6} for the optimal solution. Furthermore, the upper bounds on the SSV constraints Eq. (11) were computed using the same software package.[14]

A fine discretization in frequency for the controller and SSV constraints Eqs. (10) and (11) will result in a (possibly very) large number of constraints. In this study, robust stability of the second mode was enforced by only considering a narrow frequency range for the SSV constraints, just covering the corresponding peak in Fig. 4. When the same approach is used for the controller constraints, a problem with about 10 constraints was obtained. The optimal solution was found to be quite sensitive to the discretization of the SSV constraints, and a frequency resolution of 0.001 Hz was used. For the controller constraints, a resolution of 0.1 Hz proved sufficient. Finally, only the closed-loop p–k eigenvalue corresponding to the second mode was constrained. The consequences of not constraining the first mode are described in the next section.

The optimization was initiated at the robust critical speed $V_{\text{rob}} = 13.5$ m/s with $\boldsymbol{x} = \boldsymbol{0}$ and $z = 0$ as initial values for the design variables. A 0.02-m/s step in airspeed was chosen, and the initial values for each optimization was obtained by linear extrapolation based on the two earlier optimal solutions. By this, a quite efficient scheme was obtained, and each optimization problem was solved in a few iterations.

Results

The sequence of optimization problems were solved up to $V = 25$ m/s, from which a continuous optimal control law $\boldsymbol{x}^*(V)$ was obtained from the discrete solutions $\boldsymbol{x}_i^*(V_i)$ by linear interpolation. For brevity, the optimal controller is presented in terms of the required control power $||\boldsymbol{K}[p, x^*(V)]||_\infty$ in Fig. 5. Note that the wing seems to be the most sensitive to the aerodynamic uncertainty for moderate speeds, because the maximum control power is required at $V = 15.6$ m/s. For higher speeds, less control is required, which is in agreement with the trend of the real part of the open-loop eigenvalue p_2 in Fig. 2.

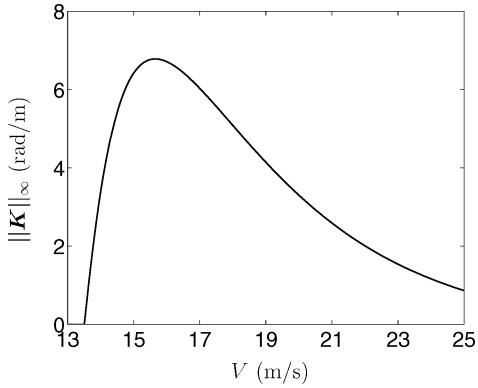

Fig. 5 Required control power vs airspeed for the optimal controller.

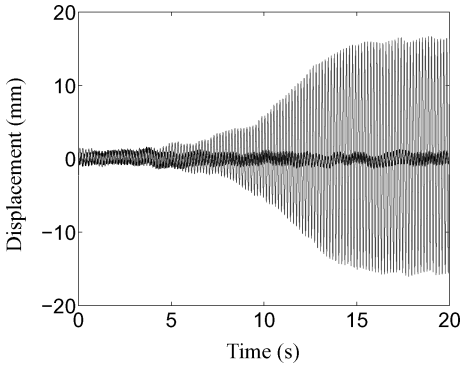

Fig. 6 Displacement of the second optical marker vs time at $V = 21.0$ m/s.

Also note that the nominal stability constraint is not active for any airspeed, meaning that the properties of the control law are depicted by the SSV constraints only. That the optimal controller actually stabilizes the plant (in theory) is verified by considering the real part of the closed-loop eigenvalues in Fig. 2 (dashed lines). Up to the robust flutter speed, the controller is not active, and the open- and closed-loop branches coalesce. However, above the robust flutter speed, the closed-loop eigenvalue corresponding to the second mode is stabilized. Clearly, the first mode is hardly affected at all by the controller. This means that the control surface motions due to the second-mode deformation only have a limited influence on the first mode. This is an interesting property of the present system, but cannot be expected in general.

The closed-loop SSV as function of frequency at $V = 21.8$ m/s is shown in Fig. 4 (dashed line). In particular, observe that the stability constraint corresponding to the second mode is active. However, also observe that, from this speed and higher, there is a potential risk for a flutter instability in the first mode. This is not taken into account in the optimization, and a robust stability analysis of the closed-loop plant, thus, predicts a potential aeroservoelastic instability in the 3.3-Hz range from $V = 21.8$ m/s and higher.

The optimal controller was digitized in the experiment using Tustin's approximation (see Ref. 6), and linear interpolation was used for scheduling the optimal feedback gains with airspeed. Encouragingly enough, the controller was found to stabilize the second-mode flutter, and a divergence instability occurred at $V = 22.7$ m/s in the experiment. Computing a robust divergence speed is not part of the present study because such an analysis would have to consider real valued perturbations to the aerodynamic forces and requires additional experimental data for model validation.

The response of the displacement of the second optical marker (Fig. 1) at $V = 21.0$ m/s is shown vs time in Fig. 6. With active control, the response is seen as a small limit-cycle oscillation with an amplitude of the order of 1 mm. This residual motion has been observed in previous studies[7] and is due to a small play in the servomechanism and a limited resolution in the optical measurements. If the control system is turned off, the amplitude slowly increases until a limit-cycle oscillation with an amplitude of roughly 16 mm develops. The control system was also capable of regaining stability if turned on again. In fact, at this airspeed, the present controller is capable of suppressing the flutter instability using approximately 75% less control power compared to the controller used by Borglund and Kuttenkeuler.[7] The results are also consistent with those arrived at by Borglund.[15] To summarize, the robust control law design was successful.

Conclusions

The present study has demonstrated the possibility to tailor the properties of an aeroservoelastic system subject to a detailed uncertainty description. It appears as if SSV analysis is a promising path toward the formulation and solution of multidisciplinary optimization problems considering uncertainties. However, the straightforward problem formulation considered in this paper, involving constraints on eigenvalues and computable bounds on structured singular values, is rather simple and nonsmooth. The development of improved problem formulations emphasizing well-behaved objective and constraint functions is of vital importance to take full advantage of gradient-based optimization for robust optimal design. The development of an efficient and accurate sensitivity analysis with respect to an arbitrary set of design variables is also a substantial part of this work. The importance of further development of uncertainty descriptions for the major disciplines, as well as methods for model validation, cannot be underestimated. Nevertheless, the results obtained in this study are encouraging, although further case studies are required to gain confidence in robust multidisciplinary design optimization in practice.

Acknowledgments

The National Program for Aeronautics Research is gratefully acknowledged for financial support.

References

[1]Lind, R., and Brenner, M., *Robust Aeroservoelastic Stability Analysis,* Springer-Verlag, London, 1999, pp. 1–5, 21–22.

[2]Kuttenkeuler, J., and Ringertz, U. T., "Aeroelastic Design Optimization with Experimental Verification," *Journal of Aircraft*, Vol. 35, No. 3, 1998, pp. 505–507.

[3]Waszak, M. R., "Robust Multivariable Flutter Suppression for Benchmark Active Control Technology Wind-Tunnel Model," *Journal of Guidance, Control, and Dynamics*, Vol. 24, No. 1, 2001, pp. 147–153.

[4]Moulin, B., Idan, M., and Karpel, M., "Aeroservoelastic Structural and Control Optimization Using Robust Design Schemes," *Journal of Guidance, Control, and Dynamics*, Vol. 25, No. 1, 2002, pp. 152–159.

[5]Borglund, D., "Robust Aeroelastic Stability Analysis Considering Frequency-Domain Aerodynamic Uncertainty," *Journal of Aircraft*, Vol. 40, No. 1, 2003, pp. 189–193.

[6]Stevens, B. L., and Lewis, F. L., *Aircraft Control and Simulation,* Wiley, New York, 1992, pp. 115–117, 547–549, 565–567.

[7]Borglund, D., and Kuttenkeuler, J., "Active Wing Flutter Suppression Using a Trailing Edge Flap," *Journal of Fluids and Structures*, Vol. 16, No. 3, 2002, pp. 271–294.

[8]Bäck, P., and Ringertz, U. T., "Convergence of Methods for Nonlinear Eigenvalue Problems," *AIAA Journal*, Vol. 35, No. 6, 1997, pp. 1084–1087.

[9]Kumar, A., and Balas, G. J., "An Approach to Model Validation in the μ Framework," *Proceedings of the American Control Conference*, Baltimore, MD, June 1994, pp. 3021–3026.

[10]Packard, A., and Doyle, J., "The Complex Structured Singular Value," *Automatica*, Vol. 29, No. 1, 1993, pp. 71–109.

[11]Seyranian, A. P., "Sensitivity Analysis of Multiple Eigenvalues," *Mechanics of Structures and Machines*, Vol. 21, No. 2, 1993, pp. 261–284.

[12]Packard, A., and Pandey, P., "Continuity Properties of the Real/Complex Structured Singular Value," *IEEE Transactions on Automatic Control*, Vol. 38, No. 3, 1993, pp. 415–428.

[13]Branch, M. A., and Grace, A., "MATLAB Optimization Toolbox User's Guide," MathWorks, Natick, MA, 1996.

[14]Balas, G. J., Doyle, J. C., Glover, K., Packard, A., and Smith, R., "μ-Analysis and Synthesis Toolbox User's Guide," MathWorks, Natick, MA, 1996.

[15]Borglund, D., "Aeroservoelastic Design Optimization with Experimental Verification," *Journal of Aircraft*, Vol. 38, No. 5, 2001, pp. 958–961.